

Universal Scaling of Hyperfine-Induced Electron Spin Echo Decay

Neil Shenvi, Rogerio de Sousa, and K. Birgitta Whaley

*Department of Chemistry and the Kenneth S. Pitzer Center for Theoretical Chemistry,
University of California, Berkeley, Berkeley, CA 94720*

(Dated: February 8, 2020)

The decoherence of a localized electron spin in a lattice of nuclear spins is an important problem for potential solid-state implementations of a quantum computer. We demonstrate that even at high fields, virtual electron spin-flip processes due solely to the hyperfine interaction can lead to complex nuclear spin dynamics. These dynamics, in turn, can lead to single electron spin phase fluctuation and decoherence. We show here that remarkably, a spin echo pulse sequence can almost completely reverse these nuclear dynamics except for a small visibility loss, thereby suppressing contribution of the hyperfine interaction to T_2 processes. For small systems, we present numerical evidence which demonstrates a universal scaling of the magnitude of visibility loss that depends only on the inhomogeneous line width of the system and the magnetic field.

PACS numbers: 03.67.Lx, 03.65.Yz, 76.60.Lz, 76.30.-v

I. INTRODUCTION

The hyperfine coupling between an excess electron spin and its surrounding nuclear spin lattice is an important source of decoherence in spin-based quantum dot schemes for solid state quantum computation [1, 2]. Due to the hyperfine coupling, the Zeeman energy of the electron spin can be exchanged with the Overhauser energy of the nuclear lattice, resulting in loss of longitudinal electron spin polarization. In addition, time fluctuations of the Overhauser field lead to loss of coherence of the electronic spin state[3]. In a Si based quantum computer, it may be possible to avoid this interaction by using isotopically purified Si (^{28}Si has no nuclear spin) [3, 4]. However, for many III-V semiconductors such as GaAs, there are no spin-zero nuclear isotopes; therefore the influence of the hyperfine coupling will have to be taken into account. A comprehensive understanding of the hyperfine interaction may allow the loss of electron spin coherence to be minimized through intelligent hardware design or pulse sequence engineering.

Numerous studies have investigated the electron spin decay induced by the hyperfine interaction under free evolution. At zero external field, calculations of the exact quantum dynamics for small systems established that the hyperfine interaction generates substantial entanglement between the electron and the nuclear spin lattice [5]. At low external fields, analytic solutions were obtained to describe the decay of electron spin correlation functions, finding that longitudinal spin relaxation occurs via power law decay on a timescale governed by $A\sqrt{N}$ where N is the number of nuclei and A is the average hyperfine coupling strength[2, 6]. A generalized master equation has also been used to describe electron dynamics in both the high- and low-field regimes at short timescales, again finding a power law decay of coherence[7]. However, semi-classical calculations have shown that correlation functions exhibit long timescale, oscillatory behavior rather than chaotic dynamics, suggesting that correlation function decay is due to averaging over initial conditions rather than from inherent system ergodicity [8]. In all of these previous publications, electron spin decay was studied under free evolution. However, in most experiments [9, 10] and in the context of controlled spin dynamics for quantum computation, it is desirable to measure coherence in the context of a spin echo pulse sequence. Therefore, in this paper, we will investigate electron spin coherence and nuclear spin dynamics due to the hyperfine coupling under an idealized spin echo experiment. Because we are interested specifically in the effect of the hyperfine interaction, we will neglect other effects such as dipolar nuclear-nuclear coupling which can also contribute to decoherence, in order to isolate the effect of the hyperfine interaction [11].

Rather than resort to approximation methods, we simulate the full electron-nuclei system through exact diagonalization. Due to the exponential growth of the Hilbert space, only small numbers of nuclear spins can be treated using this method. However, even for small systems we observe complex dynamics which will serve to illustrate the fundamental physics for larger systems. We focus mainly on the regime of high magnetic fields in which the external magnetic field is greater than the total Overhauser field of the nuclei. This regime is both experimentally realizable and practically desirable for applications in quantum computation, since single spin measurement requires a high effective magnetic field [12]. In this high field regime, we obtain several non-intuitive results that have implications for electron spin coherence. First, we find that even at high magnetic fields, rich nuclear dynamics can still occur. Because high magnetic fields suppress single flip-flops between the electron and a nucleus, it might be naively assumed that all dynamics are suppressed. However, virtual flip-flops enable nuclear dynamics to persist even at high fields. Second, as expected, we observe rapid decay of the in-plane magnetization of the electron under free evolution of the system (no spin echo), both for a pure initial state and for a completely mixed initial state. However, if we simulate a spin echo sequence, we find that the complex nuclear dynamics are almost completely reversed and the in-plane

magnetization of the electron is almost completely recovered, except for a small visibility decay. This phenomenon, if it can be generalized to larger numbers of spins, would imply that the spin echo pulse sequence can remove almost all electron decoherence caused by the hyperfine interaction. This behavior appears to reflect some partial hidden symmetry of the hyperfine Hamiltonian in the presence of an external field.

This paper is organized as follows: Section II defines our system Hamiltonian and gives background information regarding the spin echo experiment and the origin of nuclear dynamics. Section III presents our numerical results. Conclusions are presented in Section IV together with discussion.

II. BACKGROUND

In this section, we present general background information regarding our spin system. First, we will define our Hamiltonian and identify some of the symmetries we can use to simplify it. We also give a brief synopsis of decoherence processes and cite how they relate to our system. Second, we outline the spin echo experiment and discuss its utility for removing inhomogeneous contributions to the electron spin decay. Finally, we derive an effective Hamiltonian which explains the origin of the nuclear dynamics that we observe in our numerical simulations.

The system we study is that of a localized electron with spin operator \mathbf{S} in a lattice of N nuclear spins, with spin operators $\mathbf{I}_1, \mathbf{I}_2, \dots, \mathbf{I}_N$. Here we consider spin 1/2 nuclei such that $S = I = 1/2$. The system in question could be an impurity electron bound to a doping atom in a semiconductor lattice, or an excess electron in a quantum dot. The electron spin is coupled to the j^{th} nuclear spin via the hyperfine interaction A_j . The Hamiltonian for this system is [2, 5, 7, 11]

$$H = \gamma_S B S_z + \gamma_I B \sum_j I_{jz} + \sum_j A_j \mathbf{S} \cdot \mathbf{I}_j, \quad (1)$$

where γ_S and γ_I are the gyromagnetic ratios of the electron and nuclei, respectively, and B is the external magnetic field. Here, we have neglected nuclear-nuclear dipolar coupling, which is known to contribute to electron spin decoherence through nuclear spectral diffusion, because we would like to isolate the contribution of the hyperfine coupling [11, 13]. The Hamiltonian in Eq. (1) conserves the total spin angular momentum. Thus, we can immediately block diagonalize the Hamiltonian based on the $J_z = S_z + \sum_j I_{jz}$ operator. For convenience, we will label each of these blocks by the quantum number L where L is the total number of “down” spins (i.e. $J_z = N - 2L$, $L = (N - J)/2$). For a given block with quantum number L , we can then remove the nuclear Zeeman energy from the Hamiltonian by subtracting an overall constant,

$$H = (\gamma_S - \gamma_I) B S_z + E_L + \sum_j A_j \mathbf{S} \cdot \mathbf{I}_j, \quad (2)$$

where

$$E_L = \hbar \gamma_I B (N - 2L + 1). \quad (3)$$

Since each block can be treated independently, all further analysis pertains to the subspace specified by some given value of the quantum number L . In general, we will also drop E_L since it will add only an overall phase to the evolution within any given subspace.

The full Hamiltonian can be separated into a zeroth order Hamiltonian H_0 and a perturbation V ,

$$H = H_0 + V \quad (4)$$

$$H_0 = (\gamma_S - \gamma_I) B S_z + \sum_j A_j S_z I_{jz} \quad (5)$$

$$V = \frac{1}{2} \sum_j A_j (S_+ I_{j-} + S_- I_{j+}). \quad (6)$$

At high B fields, this separation can be used to gain insight into the origin of system dynamics [11]; however, it should be emphasized that we simulate here the full quantum dynamics using exact diagonalization, not by using any type of perturbative treatment. We define $|\uparrow\rangle$ and $|\downarrow\rangle$ to represent the $+z$ and $-z$ polarized electron states, respectively. We also define \mathbf{z} to be an N -bit string of $+1$'s and -1 's representing a given state of the nuclei in the z basis. The eigenstates of the unperturbed Hamiltonian, H_0 , are then given by $|\uparrow, \mathbf{z}\rangle$ or $|\downarrow, \mathbf{z}\rangle$.

In such a system, the electron spin undergoes decoherence processes, which are usually described by the Bloch equations and which are usually characterized by coherence timescales T_1 and T_2 . However, the Bloch equations

assume an exponential form for coherence decay which is not a valid assumption for hyperfine-induced decay [2, 7]. If we wish to characterize the timescale of decoherence, we must select a suitable definition for T_1 and T_2 . In this paper, we define T_1 to be the time it takes for the longitudinal electron spin magnetization $S_z(t)$ to decay to $1/e$ of its initial value. Similarly, we define T_2^* to be the time it takes for the magnitude of the in-plane magnetization $S_+(t)$ to decay to $1/e$ of its initial value. T_2^* contains contributions from inhomogeneous broadening, which results either from the measurement of an ensemble of spins in different local environments, or from the measurement of a single spin in a mixed initial state, $\rho(0)$. Therefore we also define the spin echo coherence time T_2 , which is defined as the time it takes for the spin echo envelope to decay to $1/e$ of its initial value [14]. T_2 contains no contributions from inhomogeneous broadening, which is removed by the spin echo pulse sequence. These definitions are equivalent to the standard definitions in the case of exponential decay.

We now note that due to the large Zeeman energy of the electron, there will be an energy gap between the manifold of electron spin-up and electron spin-down eigenstates of H_0 . It is clear that for large enough fields, T_1 will be infinite because there is then no efficient mechanism for the longitudinal relaxation of the electron spin. If we define the total Overhauser field,

$$B_c = \frac{\hbar}{\gamma_S - \gamma_I} \sum_j A_j \quad (7)$$

then when $B > B_c$ we can derive several results[11]:

1. The S_z label is approximately a good label for the eigenstates of H . In other words, eigenstates of H are either nearly electron spin-up ($|\uparrow\rangle$) or nearly electron spin-down ($|\downarrow\rangle$). We will refer to these states as “+” and “-” eigenstates, respectively.
2. There is an energy gap of approximately $\hbar\gamma_S B$ between nearly spin-up (“+”) eigenstates of H and nearly spin-down (“-”) eigenstates of H .
3. Because S_z is nearly a good label for the eigenstates of H , $S_z(t)$ can only deviate a small amount from its initial value,

$$|S_z(t) - S_z(0)| \leq \mathcal{O}\left(\frac{B_c^2}{B^2}\right). \quad (8)$$

Hence, we can identify B_c as a critical field for the longitudinal relaxation of the system. (Results 1-3 are proved rigorously in [11].)

Although longitudinal relaxation is suppressed at high fields, resulting in an infinite value for the T_1 coherence time, the same is not necessarily true for the intrinsic in-plane coherence time, T_2 . In fact, numerical evidence (see Sec. III) demonstrates that T_2 is governed by a second critical field, Δ_c , defined as,

$$\Delta_c = \frac{\hbar}{\gamma_S - \gamma_I} \sqrt{\sum_j A_j^2}. \quad (9)$$

Since we are concerned here with the in-plane relaxation of the electron spin, from now on when we speak of the “critical field” we will be referring to Δ_c . This critical field is equivalent to the inhomogeneous broadening linewidth due to the hyperfine interaction (i.e., $T_2^* \sim 1/(\gamma_S \Delta_c)$). What is remarkable, however, is that this quantity also acts as a critical field for *intrinsic* broadening.

This intrinsic broadening (T_2) can be caused by nuclear dynamics which stem from second-order spin flip processes. Because these second-order processes conserve S_z , they are not suppressed as strongly as T_1 processes. It is these second-order processes which cause the divergences in second-order perturbation theory noted in [2]. In addition to intrinsic broadening, inhomogeneous broadening which contributes to T_2^* can occur in an ensemble measurement when an ensemble of electrons is subjected to a slightly inhomogeneous magnetic field. Inhomogeneous broadening can also occur when a single electron experiences an ensemble of Overhauser fields due to the nuclei being in a mixed state. In our calculations, inhomogeneous broadening will result from the use of a fully mixed initial state for the nuclear spins. This static, inhomogeneous contribution to T_2^* can be contrasted to the dephasing induced by dynamic sources, such as a time-varying external field or a fluctuating nuclear Overhauser field caused by nuclear spin dynamics. To remove the contribution due to static, inhomogeneous broadening and recover the intrinsic coherence time, T_2 , we must perform a spin echo sequence ($\pi/2 - \tau - \pi - \tau$ -echo).

We now turn our attention to a detailed analysis of the spin echo experiment for this system, which will be crucial in interpreting our numerical results. The spin echo experiment was developed by Hahn [14] to remove inhomogeneous

broadening in an ensemble spin measurement. We will assume that at the beginning of the spin echo experiment, the electron spin has been rotated to point in the $+x$ direction. The system is then allowed to evolve freely for some time τ . Next, an idealized π -pulse which flips the spin of the electron is applied. The π pulse is described by the operator,

$$R_\pi = |\uparrow\rangle\langle\downarrow| + |\downarrow\rangle\langle\uparrow|. \quad (10)$$

After another period of free evolution for time τ , the magnitude of the in-plane magnetization of the electron, $S_+ = (S_x + iS_y)/2$, is measured, yielding a measure of single spin coherence.

In addition to removing the effects of inhomogeneous broadening, the spin echo experiment can remove dephasing due to a broad class of Hamiltonians having the form,

$$H_{se} = |\uparrow\rangle\langle\uparrow| \otimes V_\uparrow + |\downarrow\rangle\langle\downarrow| \otimes V_\downarrow, \quad (11)$$

where V_\uparrow and V_\downarrow are arbitrary operators on the nuclear spins that have the commutation property $[V_\uparrow, V_\downarrow] = 0$. The in-plane magnetization after the spin echo sequence is given by

$$\langle \tilde{S}_+(\tau; \tau) \rangle = \text{Tr} [\rho(0) U^\dagger(\tau) R_\pi U^\dagger(\tau) S_+ U(\tau) R_\pi U(\tau)], \quad (12)$$

where

$$U(\tau) = e^{iH_{se}\tau/\hbar}. \quad (13)$$

First we note that we can write H_{se} as

$$H_{se} = (V_\uparrow + V_\downarrow) \mathcal{I} + (V_\uparrow - V_\downarrow) S_z. \quad (14)$$

Then we note the relations,

$$R_\pi S_z R_\pi = -S_z \quad (15)$$

$$R_\pi S_+ R_\pi = S_-. \quad (16)$$

Using these facts, we find that

$$\langle \tilde{S}_+(\tau; \tau) \rangle = \text{Tr} [\rho(0) U^\dagger(\tau) R_\pi U^\dagger(\tau) S_+ U(\tau) R_\pi U(\tau)] \quad (17)$$

$$= \text{Tr} \left[\rho(0) e^{-i(V_\uparrow - V_\downarrow) S_z \tau / \hbar} R_\pi e^{-i(V_\uparrow - V_\downarrow) S_z \tau / \hbar} R_\pi S_- R_\pi e^{i(V_\uparrow - V_\downarrow) S_z \tau / \hbar} R_\pi e^{i(V_\uparrow - V_\downarrow) S_z \tau / \hbar} \right] \quad (18)$$

$$= \text{Tr} \left[\rho(0) e^{-i(V_\uparrow - V_\downarrow) S_z \tau / \hbar} e^{i(V_\uparrow - V_\downarrow) S_z \tau / \hbar} S_- e^{-i(V_\uparrow - V_\downarrow) S_z \tau / \hbar} e^{i(V_\uparrow - V_\downarrow) S_z \tau / \hbar} \right] \quad (19)$$

$$= \text{Tr} [\rho(0) S_-] \quad (20)$$

$$= \langle S_-(0) \rangle. \quad (21)$$

Hence, we arrive at the conclusion that the spin echo experiment removes decay of in-plane magnetization for all Hamiltonians of the form given in Eq. (11).

To understand the origin of nuclear dynamics in this system, we can derive an effective Hamiltonian which contains nuclear-nuclear interactions. Let $|\psi^+\rangle$ be a “+” eigenstate of the Hamiltonian, H , i.e. $|\psi^+\rangle$ has primarily electron spin-up character. Without loss of generality, $|\psi^+\rangle$ can be written as

$$|\psi^+\rangle = |\uparrow, \psi_\uparrow^+\rangle + |\downarrow, \psi_\downarrow^+\rangle. \quad (22)$$

Because the perturbation V flips the polarization of the electron, the action of H on the electron spin-up and electron spin-down subspaces yields the two simultaneous equations,

$$H_0 |\uparrow, \psi_\uparrow^+\rangle + V |\downarrow, \psi_\downarrow^+\rangle = E_+ |\uparrow, \psi_\uparrow^+\rangle \quad (23)$$

$$H_0 |\downarrow, \psi_\downarrow^+\rangle + V |\uparrow, \psi_\uparrow^+\rangle = E_+ |\downarrow, \psi_\downarrow^+\rangle. \quad (24)$$

Eq. (24) can be solved for $|\downarrow, \psi_\downarrow^+\rangle$ and the resulting expression inserted into Eq. (23) yields

$$H_0 |\uparrow, \psi_\uparrow^+\rangle + V \frac{1}{E_+ - H_0} V |\uparrow, \psi_\uparrow^+\rangle = E_+ |\uparrow, \psi_\uparrow^+\rangle. \quad (25)$$

Because of the energy gap between the spin-up and spin-down states, the operator $1/(E_+ - H_0)$ is always well-defined [11]. Because the left-hand side of Eq. (25) depends on E_+ , it is not a true Schrödinger equation; to obtain E_+ exactly, Eq. (25) must be solved self-consistently. However, if we use $E_+ \approx (\gamma_S - \gamma_I)B/2$, then we can obtain an effective Hamiltonian from Eq. (25). The effective Hamiltonian for the electron spin-up subspace is

$$H_{\text{eff}}^+ = H_0 + V_{\text{eff}}^+ \quad (26)$$

$$V_{\text{eff}}^+ = \frac{\hbar^2}{4} \sum_{j,k} A_j A_k I_{j-} \frac{1}{(\gamma_S - \gamma_I)B + \frac{1}{2}\hbar \sum_j A_j I_{jz}} I_{k+}. \quad (27)$$

We obtain a similar, but not identical, effective Hamiltonian for the spin-down subspace (note the transposition of the I_- and I_+ operators),

$$H_{\text{eff}}^- = H_0 + V_{\text{eff}}^- \quad (28)$$

$$V_{\text{eff}}^- = -\frac{\hbar^2}{4} \sum_{j,k} A_j A_k I_{j+} \frac{1}{(\gamma_S - \gamma_I)B + \frac{1}{2}\hbar \sum_j A_j I_{jz}} I_{k-}. \quad (29)$$

Eqs. (27) and (29) show that the overall coupling between nuclei does indeed decrease at high fields, because the operator $1/(E - H_0)$ scales approximately as $1/B$. However, the energy cost of flip-flopping two nuclei j and k is proportional to $A_j - A_k$. Thus, if A_j and A_k are close in value, the nuclei can flip-flop even at high fields.

If we now examine the hyperfine Hamiltonian in Eq. (1) in light of this discussion, we note that it is not immediately clear whether the spin echo experiment will remove all dephasing. H does not have the form of H_{se} given in Eq. (11). Furthermore, as noted above, although real electron spin-flip processes are suppressed at high magnetic field, the electron can instead undergo a virtual flip-flop which corresponds to the perturbation V acting twice on the initial state. This action leaves the spin state of the electron unchanged, but flip-flops the spins of two nuclei. Because this process does not produce a net change in the longitudinal polarization of the electron, it can occur even at high fields (when T_1 processes are substantially suppressed) and hence may contribute to electron spin decoherence. We will provide explicit examples of the nuclear spin dynamics resulting from these virtual electron spin flip processes in Section III.

III. NUMERICS

We now show numerical calculations for one electron and $N = 5 - 13$ nuclei. Due to the exponential size of the Hilbert space, simulating larger systems rapidly becomes unfeasible. However, even in small systems, we will see that the basic physics of the hyperfine interaction and its role in the features of the resulting nuclear dynamics become apparent. We will show that the spin echo envelope decay depends only on the ratio of the external field B to the critical field Δ_c .

We will make use of two different initial states in our simulations. The first initial state we consider is a pure state in which the nuclei are all pointed in either the $+z$ or $-z$ direction:

$$|\psi_0\rangle = |\leftarrow\rangle \otimes |\mathbf{z}_0\rangle, \quad (30)$$

where $|\mathbf{z}_0\rangle$ is a randomly chosen simultaneous eigenstate of the I_{jz} operators. Our second initial state is the completely mixed nuclear density matrix $\rho(0)$, given by

$$\rho(0) = c |\leftarrow\rangle \langle\leftarrow| \otimes \mathcal{I}_I, \quad (31)$$

where c is a normalization constant and \mathcal{I}_I is the identity operator on the nuclear spins. In both cases, the electron is initially polarized in the $+x$ direction. We simulate the nuclear dynamics for a specific set of hyperfine constants, $\{A_j\}$, where $j = 1 \dots N$ and $N = 9$. The hyperfine constants are selected randomly from a uniform distribution on the range $[.1, .2]$ Tesla yielding a total Overhauser field of $B_c = 1.42$ Tesla and a critical field of $\Delta_c = 0.482$ Tesla. Although the nuclear dynamics will depend on the specific values for the coupling constants, we show below that our key results, namely the near-reversal of nuclear dynamics and the near-absence of electron spin decoherence, are valid regardless of the particular values of the hyperfine coupling constants. Furthermore, we find that these results show little dependence on the number of nuclei N .

First, we verify that even at high fields nuclear dynamics can occur in the form of electron mediated flip-flop between nuclei. The primary observable we use to quantify nuclear spin dynamics is the overlap of the nuclear state at time t with the initial nuclear state $|\mathbf{z}_0\rangle$, which is specified by the projection operator

$$P_{\mathbf{z}_0} = |\mathbf{z}_0\rangle \langle\mathbf{z}_0|. \quad (32)$$

In the absence of nuclear flip-flop, this operator will have the value 1 for all times t . Figure 1 shows the free evolution of $P_{z_0}(t)$ at $B = 0.030, 0.121, .482, 1.93, 7.72$ Tesla (i.e., $B = \frac{1}{16}\Delta_c, \frac{1}{4}\Delta_c, \Delta_c, 4\Delta_c, 16\Delta_c$) given the initial state $|\psi_0\rangle$ defined in Eq. (30). We see clearly that above the critical field, the magnitude of nuclear dynamics decreases as the external field increases, because the coupling between nuclear states due to V_{eff} scales as $1/B$. In essence, increasing the magnetic field acts to gradually “freeze out” nuclear flip-flop.

Figure 2 shows the magnitude of $\langle S_+(t) \rangle$ for the same system. At low fields, where extensive nuclear dynamics occur, the magnitude of $\langle S_+(t) \rangle$ decays because the electron experiences a fluctuating magnetic field. This effect is very similar to what is observed in nuclear spectral diffusion[3], except that here the coupling constant between nuclei depends on the external magnetic field. As we begin to freeze out nuclear flip-flops at higher fields, the magnitude of $\langle S_+(t) \rangle$ does not decay substantially from its initial value because the electron simply precesses at some frequency governed by the initial nuclear configuration and its effective Overhauser field.

Although these simulations are useful to explore the origin of nuclear dynamics, it is important to note that in real experiments the magnitude of the in-plane magnetization of the electron, $\langle S_+(t) \rangle$, will decay even in the absence of nuclear flip-flop. In a real system the initial state is unlikely to be a z -polarized state of the nuclei, or even a pure state of the nuclei; rather, the initial nuclear density matrix will likely be highly mixed. In other words, the initial density matrix will contain incoherent contributions from a variety of initial nuclear states. Even if the *magnitude* of $\langle S_+ \rangle$ undergoes no decay for each of these initial nuclear states, the frequency of precession for each initial state will be different, leading to overall dephasing. This dephasing is what is normally known as “inhomogeneous broadening”; it is not necessarily intrinsic to the system but is only due to the mixed initial state. Thus, it becomes necessary to use the spin echo experiment to remove this inhomogeneous decay and to recover the intrinsic decay constant T_2 . To investigate this effect, we will now use a fully mixed nuclear density matrix as an initial state (see Eq. (31)).

First, we confirm that a mixed initial state does indeed lead to inhomogeneous broadening in our system. Figure 3 shows that, as expected, the ensemble of Overhauser fields experienced by the electron due to the mixed initial nuclear state leads to dephasing on a timescale that is nearly independent of the external field. We also see that at high fields, the mixed initial state leads to a faster decay of $|\langle S_+(t) \rangle|$ than the pure initial state, due to the presence of both intrinsic and inhomogeneous broadening ($T_2^* < T_2$).

We now consider the dynamics of this system under the spin echo experiment. As discussed above, because H does not have the form given in Eq. (11), we do not necessarily expect the spin echo experiment to remove all dephasing. Figures 1 and 2 confirmed that for a pure initial state at $B = 0.482$ Tesla, this system undergoes both nuclear flip-flop and in-plane magnetization decay. However, Figure 4 demonstrates that if we now perform a spin echo experiment, we obtain the remarkable result that when $B \geq \Delta_c$, nearly the full magnitude of the in-plane magnetization is recovered by the spin echo pulse sequence. It might be expected that when nuclear flip-flop is “frozen out” at very high fields (for instance, at $B = 7.72$ Tesla), the spin echo experiment will reverse nearly all in-plane magnetization decay. However, it is surprising that in systems at much lower fields, for which more complex nuclear dynamics occur, the same reversal of decay takes place. In fact, nuclear flip-flop dynamics due to dipolar nuclear coupling are known to be responsible for irreversible nuclear spectral diffusion [3, 15]. Yet the simulation in Figure 4 shows that in contrast to this known behavior for dipolar couplings, *the analogous nuclear dynamics induced by the hyperfine interaction do not lead to irreversible spin echo envelope decay, except for a small visibility loss.*

To probe this effect, we can directly examine the operators $S_+(\tau)$ and $\tilde{S}_+(\tau'; \tau)$. Figures 5a,b, and c show the matrix representation of the operator $S_+(\tau)$ at $\tau = 0, .1, 100000$ ns, for the block connecting electron spin down to electron spin up states. At $t = 0$, the operator $S_+(0)$ acts as the identity on the nuclear states and there are no off-diagonal contributions. However, as time evolves, nuclear dynamics, which lead to dephasing, can be clearly seen in the non-trivial action of $S_+(\tau)$ on the nuclear states, as evidenced by the increasing off-diagonal structure in Figures 5a-c. Next, a π -pulse is applied at $\tau = 100000$ ns. Figures 5d and e then show the matrix representation of the operator $\tilde{S}_+(\tau'; 100000 \text{ ns})$ at $\tau' = 99999.9, 100000$ ns. The evolution of the operator runs backwards after the application of the π -pulse, so that at $\tau' = 100000$ ns, we find that $\tilde{S}_+(\tau'; 100000 \text{ ns})$ is nearly equal to $S_+(0)$. Because the operator $\tilde{S}_+(\tau; \tau)$ is nearly the identity operator with respect to the nuclear states, the in-plane magnetization will remain close to its initial value, regardless of the initial state.

We now examine the importance of the specific values of the hyperfine constants, A_j , for this nuclear dynamics reversal to occur. So far, we have offered no justification for our particular selection of hyperfine constants, which were chosen at random from a uniform distribution. Because the nuclear and electronic dynamics depend on the exact value of the hyperfine constants, the absence of spin decay that we observe might be highly system dependent. To probe this issue, we will evaluate the magnitude of the spin-echo decay as a function of B for a variety of system parameters and sizes. For each system, we select hyperfine constants from the uniform distribution on the interval $[0, .6]$ Tesla and evaluate the time-averaged magnitude of the spin-echo envelope or the *visibility loss*, v , where

$$v = 1/2 - |\langle \tilde{S}_+(\tau; \tau) \rangle|. \quad (33)$$

In Eq. (33) the time average is taken over some suitably long time interval (approximately 500ns for our systems). Figure 6 shows a graph of the results for several values of N , where we have scaled our results to the critical field of each system (because the A_j 's were selected randomly, the critical field for each system varies). These plots clearly demonstrate a universal scaling of visibility (i.e. the magnitude of the spin echo envelope) with magnetic field, regardless of the particular values of the hyperfine coupling constants. Instead, the visibility of a given system depends only its critical field Δ_c . Furthermore, we see that this behavior is independent of system size; at external fields greater than Δ_c , the visibility loss scales as $(\Delta_c/B)^2$ for every value of N simulated. That this time-reversal phenomenon seems to be completely independent of the specific values of the hyperfine constants A_j and of the number of nuclei is remarkable, considering that the nuclear dynamics themselves are very sensitive to the particular values of A_j .

IV. DISCUSSION AND CONCLUSIONS

We have studied here the dynamics of a system of one electron interacting with N nuclei via the hyperfine interaction with exact diagonalization methods. We have found that even at external magnetic fields above the critical field Δ_c , nuclear dynamics can still occur as a result of the second-order coupling between nuclei induced by the electron-nuclear hyperfine interaction. These dynamics cause the electron to experience a fluctuating Overhauser field, giving rise to decoherence similar to the effect of dipolar nuclear spectral diffusion. However, unlike nuclear spectral diffusion, these flip-flop dynamics due to the hyperfine interaction can be nearly completely reversed using a single spin echo pulse sequence. This reversal of nuclear dynamics in turn reverses the decay of the in-plane electron spin magnetization, leading to a negligible decay of the spin echo envelope function. The latter appears to be better characterized as a visibility loss[4]. Finally, we have found that this loss of visibility obeys a universal scaling with the external magnetic field that depends only on the critical field of the system.

It should be noted that the entanglement generated by the hyperfine interaction between the electron and nuclei has already been studied at zero external field, where it was concluded that it will be necessary to remove or at least to minimize this entanglement in a quantum computer implementation based on electron spins in solids [5]. Our investigation shows that the spin echo pulse sequence accomplishes precisely this task by reversing the dynamics of the system. Furthermore, we demonstrate that this reversal is possible at all field strengths above Δ_c , apart from a small loss of visibility on the order of $(\Delta_c/B)^2$.

Several points merit further discussion. The first is the impact of the observed universal scaling on the so-called “visibility problem” discussed by Yablonovitch et al. [4]. In that paper, the authors point out that even small scale fluctuations (i.e. loss of visibility) in the spin-echo signal caused by the electron-nucleus hyperfine interaction can be fatal to quantum computation if they are above the error threshold ($10^{-4} - 10^{-6}$). Thus, even if the spin echo experiment recovers *most* of the in-plane coherence, it is important to know how large the external magnetic field must be before the loss of in-plane coherence is below the error threshold for quantum computation. Because the critical field is shown here to scale approximately as $\Delta_c = B_c/\sqrt{N}$, for large numbers of nuclei the critical field will be substantially lower than the total Overhauser field of the nuclei. For instance, the total Overhauser field of an electronic impurity in GaAs is approximately $B_c = 2.24$ Tesla; however, the critical field is only $\Delta_c = 1.25 \times 10^{-3}$ Tesla, since there are approximately $N = 10^6$ nuclei interacting with the electron[11]. Hence, an external field of $B = 1$ Tesla would lead to a spin echo visibility loss on the order of 10^{-6} and for any field larger than this would therefore be sufficient to allow fault tolerant quantum computation (in the absence of other decoherence mechanisms).

Second, we should point out the relationship between spin coherence recovery and entanglement. Eqs. (26–29) show that spin-up states and spin-down states evolve via different effective Hamiltonians. Because the evolution of the nuclear spins depends on the state of the electron spin, the nuclei become entangled with the electron, resulting in a loss of electron spin coherence. As we have shown, the spin echo sequence reverses this loss of entanglement almost completely. In other words, the effect of the spin echo sequence can be understood as disentangling the electron spin from the nuclear spins. That the hyperfine interaction should generate entanglement is well-known [5]; what is interesting and new from the current study is that the spin echo sequence should be able to so effectively remove this entanglement.

Finally, we turn to the question of the origin of the observed universal scaling. It is our belief that such a universal scaling which is invariant to both system size and the choice of coupling constants must result from a hidden near symmetry in the system. A hidden symmetry might also account for the oscillatory behavior and long timescale persistence of spin correlation functions observed in [8]. This claim can perhaps be better understood by an analogy. The absence of longitudinal decay at high magnetic fields can be thought of as a result of the near-commutation of H and S_z . As a result of this near-commutation, S_z is a “almost” a good quantum number for the system and the longitudinal component of the electron spin decays only a small amount. In this paper, we have observed that the in-plane component of the electron spin decays only a small amount under the spin echo experiment. This fact

suggests that there might be some operator which nearly commutes with H , leading to a similar suppression of decay. The difference between the two cases is that T_1 suppression is linked to the energy gap between up and down electron spin states. There is no obvious analogous energy gap for T_2 processes, because these processes conserve electron spin. It is known that the hyperfine Hamiltonian in Eq. (1) commutes with a set of operators discovered by Gaudin [16, 17]. However, this fact does not immediately explain the presence of the observed universal scaling, nor the near-complete spin echo reversal.

Much future work remains to be done on this problem. The most obvious question that remains unanswered is the identity of the conjectured hidden symmetry and the mechanism by which it suppresses spin echo decay. This symmetry might be the one mentioned above, or it might be one that is completely new. In either case, determining its effect on the spin echo envelope would provide fascinating insight into the nature of spin dynamics.

In conclusion, we provide numerical evidence that a spin echo sequence is able to remove a substantial part of the hyperfine induced entanglement of a single electron spin interacting with a bath of nuclear spins. At high magnetic fields ($B \gg \Delta_c$) this residual entanglement reveals itself as a universal visibility loss, which is shown to depend only on the (Δ_c/B) ratio (see Eq. (9)).

Acknowledgements. We acknowledge support from the DARPA SPINS program and ONR under grant No. FDN001-01-1-0826.

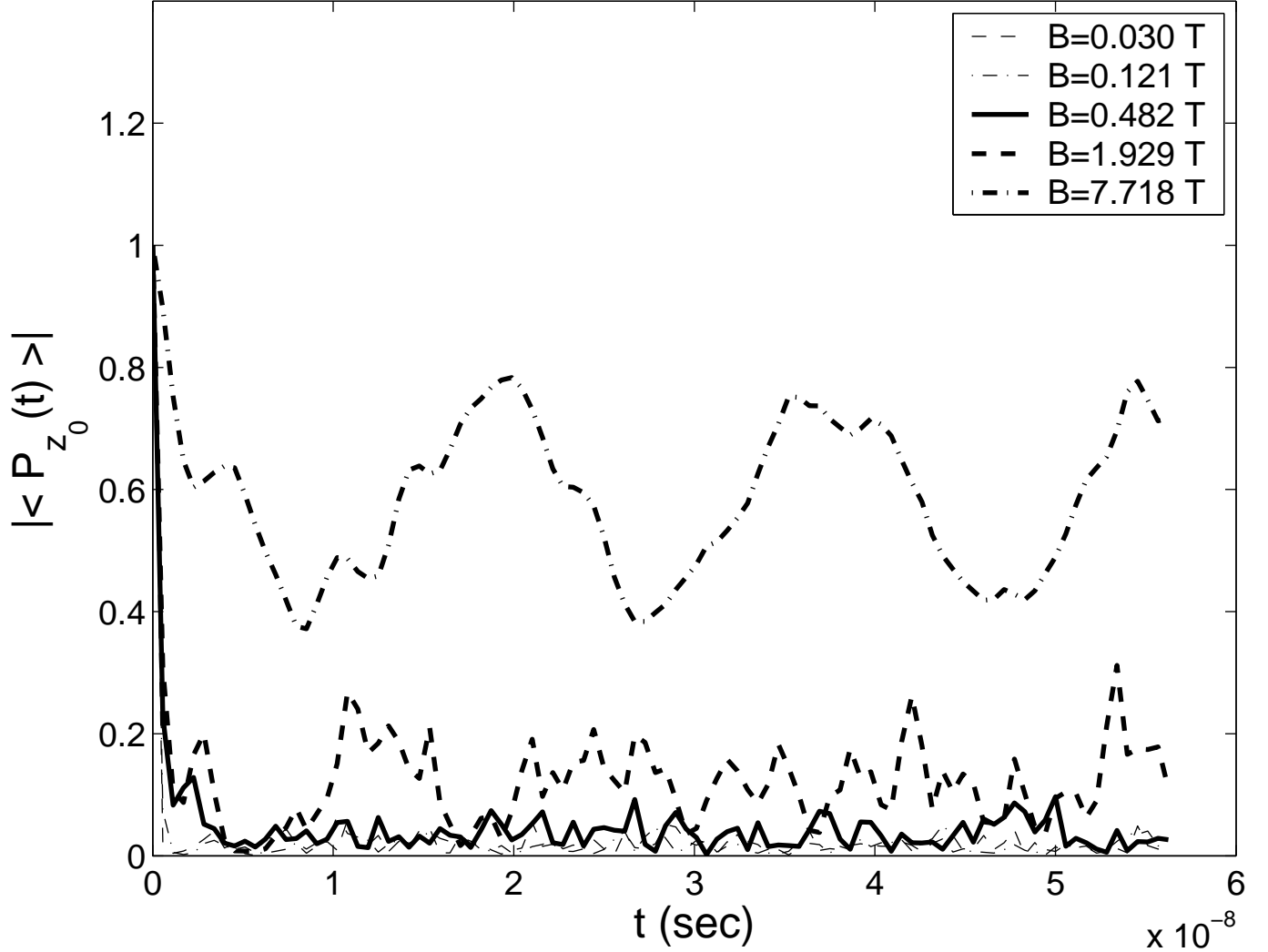


FIG. 1: The expectation value of $P_{\mathbf{z}_0} = \mathcal{I}_S \otimes |\mathbf{z}_0\rangle \langle \mathbf{z}_0|$ as a function of t at $B = 0.030, 0.121, .482, 1.93, 7.72$ Tesla for the initial state $|\psi_0\rangle$ (see Eq. (30)). In this example $N = 9$ and $\Delta_c = .482$ Tesla. As the external field increases, nuclear dynamics is slowly “frozen out”. However, nuclear dynamics clearly persist well above the critical field.

-
- [1] D. Loss and D. DiVincenzo, *Physical Review A* **57**, 120 (1998).
 - [2] A. V. Khaetskii, D. Loss, and L. Glazman, *Physical Review Letters* **88** (2003).
 - [3] R. de Sousa and S. Das Sarma, *Physical Review B* **68** (2003).
 - [4] E. Yablonovitch, H. Jiang, H. Kosaka, H. D. Robinson, D. S. Rao, and T. Szkopek, in *Proc. of the IEEE* (2003), vol. 91, pp. 761–780.
 - [5] J. Schliemann, A. V. Khaetskii, and D. Loss, *Physical Review B* **66** (2002).
 - [6] A. Khaetskii, D. Loss, and L. Glazman, *Physical Review B* **67** (2003).
 - [7] W. A. Coish and D. Loss, *cont-mat/0405676* (2004).
 - [8] S. I. Erlingsson and Y. V. Nazarov, *Physical Review B* **70**, 205327 (2004).
 - [9] A. M. Tyryshkin, S. A. Lyon, A. V. Astashkin, and A. M. Raitsimring, *Physical Review B* **68** (2003).
 - [10] E. Abe, K. Itoh, J. Isoya, and S. Yamasaki, *Physical Review B* **70**, 033204 (2004).
 - [11] N. Shenvi, R. de Sousa, and K. Whaley, *cont-mat/0410308* (2004).
 - [12] R. Hanson, B. Witkamp, L. Vandersypen, L. Willems van Beveren, J. Elzerman, and L. Kouwenhoven, *Physical Review Letters* **91** (2003).
 - [13] R. de Sousa and S. Das Sarma, *Physical Review B* **67** (2003).
 - [14] E. Hahn, *Physical Review* **80**, 580 (1950).

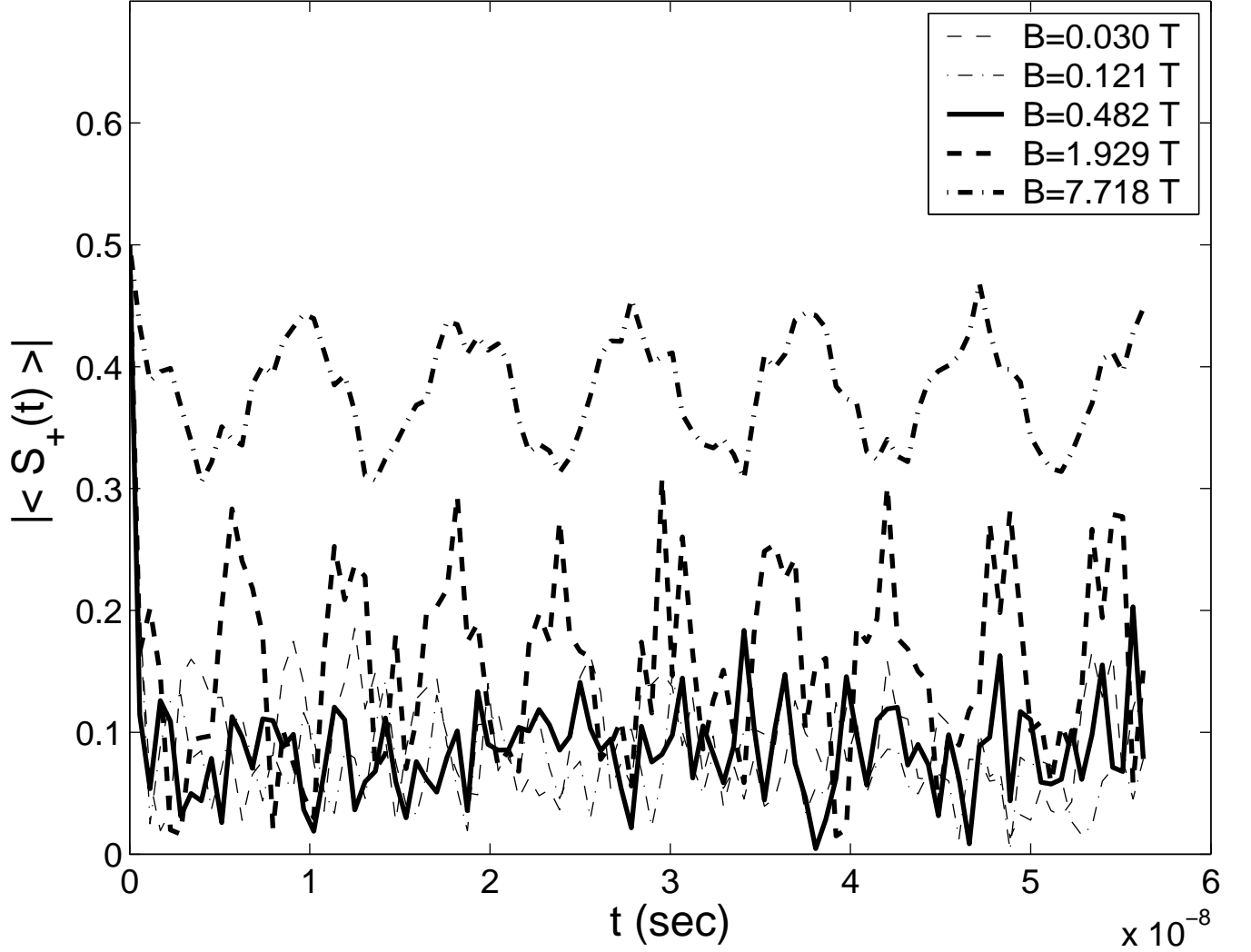


FIG. 2: The expectation value of the magnitude of the in-plane magnetization $|\langle S_+(t) \rangle|$ as a function of t at $B = 0.030, 0.121, .482, 1.93, 7.72$ Tesla for the same system as in Figure 1, i.e. the initial state is again the pure state $|\psi_0\rangle$. As the nuclear dynamics is slowly “frozen out”, there is a corresponding decrease in the magnitude of in-plane magnetization decay.

[15] R. de Sousa, N. Shenvi, and K. B. Whaley, /cond-mat/0406090 (2004).

[16] M. Gaudin, J. Phys. (Paris) **37**, 1087 (1976).

[17] J. Schliemann, A. Khaetskii, and D. Loss, J. Phys.: Condens. Matter **15**, R1809 (2003).

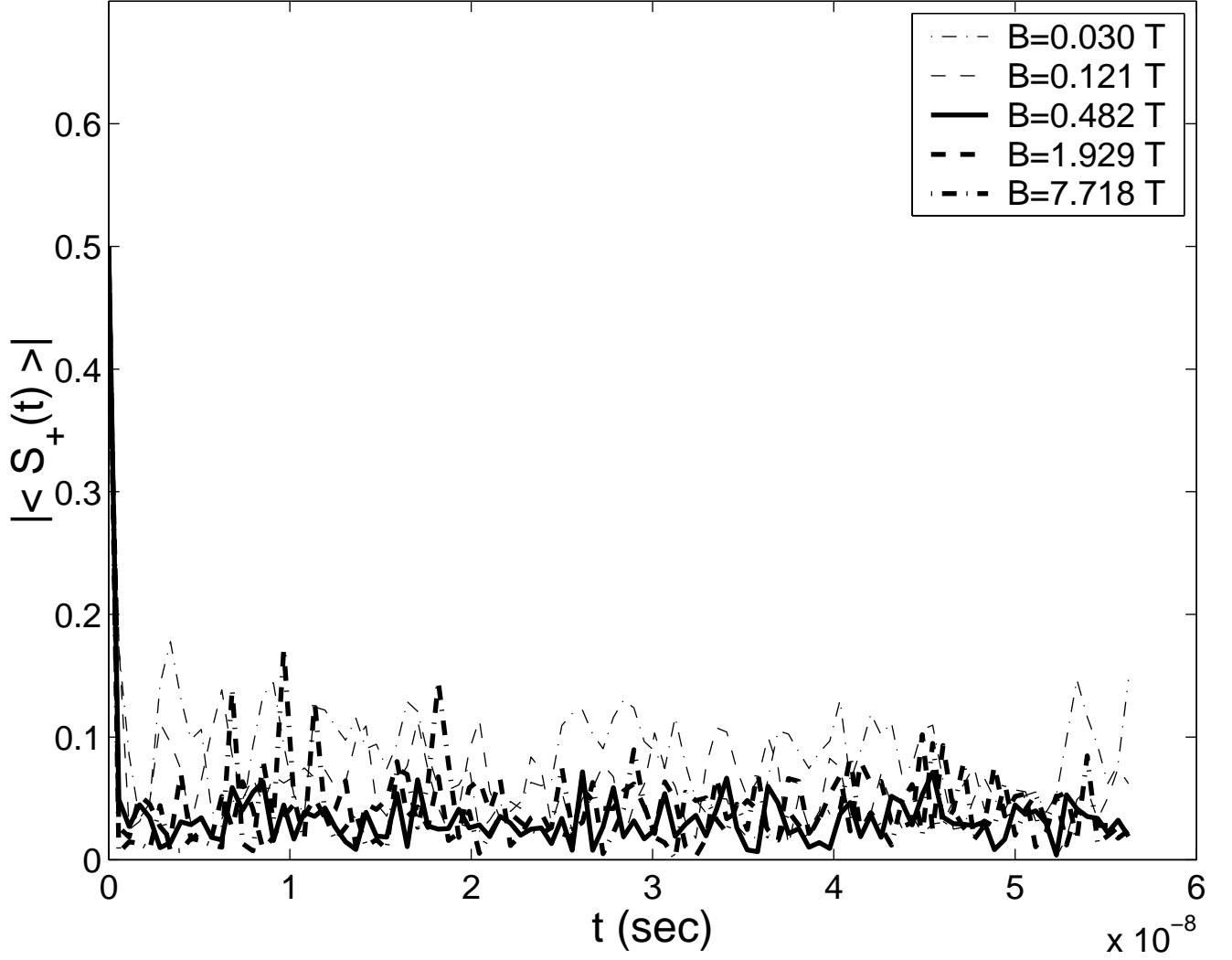


FIG. 3: The expectation value of the magnitude of the in-plane magnetization $|\langle S_+(t) \rangle|$ as a function of t at $B = 0.030, 0.121, .482, 1.93, 7.72$ Tesla for an initial density matrix $\rho(0)$ corresponding to a completely mixed nuclear state (see Eq. (31)). Inhomogeneous broadening causes the in-plane magnetization to decay on approximately the same timescale (T_2^*) independent of the external field.

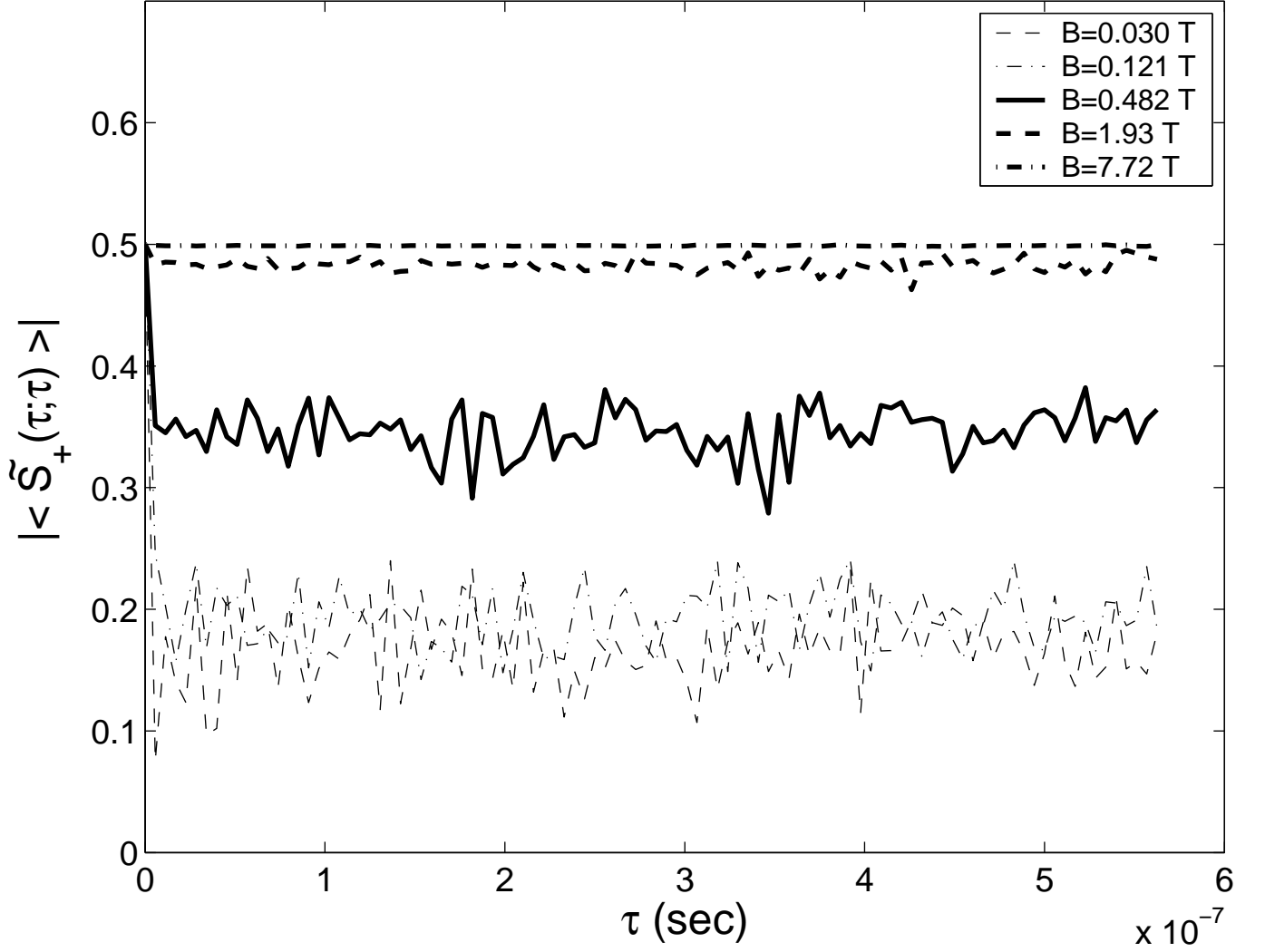


FIG. 4: The expectation value of the magnitude of the spin echo envelope $|\langle \tilde{S}_+(\tau; \tau) \rangle|$ as a function of τ at $B = 0.030, 0.121, .482, 1.93, 7.72$ Tesla. The initial nuclear state is again the mixed state specified by $\rho(0)$ (see Eq. (31)). Above the critical field Δ_c , the spin echo experiment removes nearly all decay of the in-plane magnetization, even for systems displaying substantial nuclear dynamics (i.e. $B = 1.93$ Tesla). Note that this effect persists even at long times.

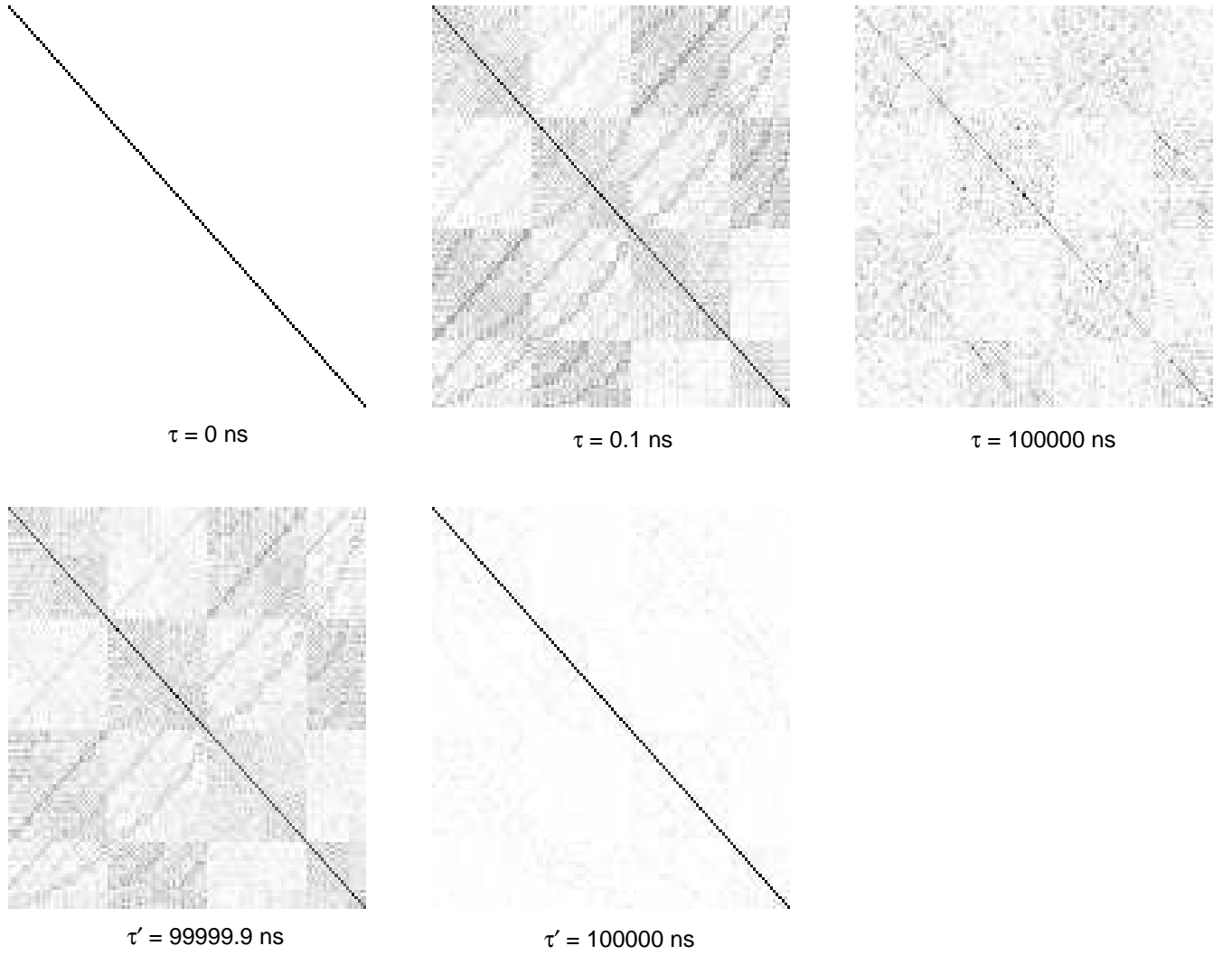


FIG. 5: The matrix representation of the operator $\tilde{S}_+(\tau'; \tau)$ at $B = \Delta_c = 0.482$ Tesla over the course of a spin echo experiment where a π -pulse is applied at $\tau = 100000$ ns. The operators are shown in the z -basis representation of the nuclear states; the intensity of each point on the plot represents the amplitude of the corresponding matrix element between nuclear states. For clarity, we consider only the primary contributing block of the operator (i.e. the block connecting electron spin down to electron spin up states) as the other blocks are much smaller in magnitude. At short times, nuclear dynamics are negligible. At longer times, nuclear dynamics are substantial, leading to potential decay of S_+ . However, the final panel shows that the spin echo experiment nearly reverses all nuclear dynamics, leading to a recovery of in-plane magnetization.

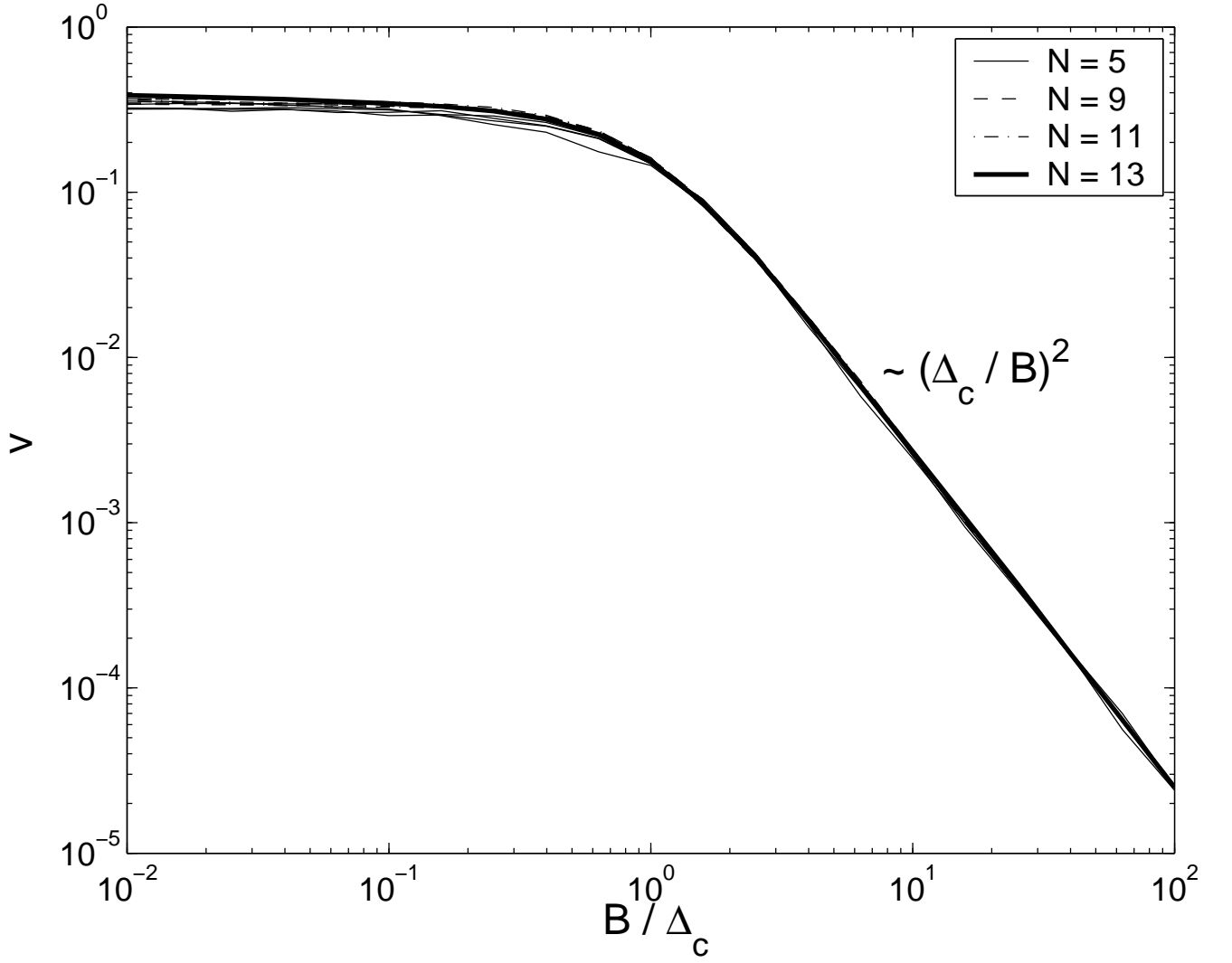


FIG. 6: The universal scaling of visibility loss, v , (see Eq. (33)) versus external field, B/Δ_c , evaluated for systems of $N = 5$, $N = 9$, $N = 11$, $N = 13$ with randomly generated sets of hyperfine coupling constants. Five systems were simulated for the system sizes $N = 5$, $N = 9$, and $N = 11$. Only one system was simulated for $N = 13$ because the large size of the system required substantial computation time (approximately five days on a multiple-node workstation). Above the critical field $B > \Delta_c$, the visibility loss scales as $(\Delta_c/B)^2$, independent of the selection of the hyperfine constant values and the size of the system, N .